Radiotherapy and Oncology 151 (2020) 228–233

Contents lists available at ScienceDirect

Radiotherapy and Oncology

journal homepage: www.thegreenjournal.com

Original Article

Online-adaptive versus robust IMPT for prostate cancer: How much can we gain?

Thyrza Z. Jagt [a,*], Sebastiaan Breedveld [a], Rens van Haveren [a], Ben J.M. Heijmen [a], Mischa S. Hoogeman [a,b]

[a] Department of Radiation Oncology, Erasmus MC Cancer Institute, Rotterdam; and [b] Department of Medical Physics & Informatics, HollandPTC, Delft, The Netherlands

ARTICLE INFO

Article history:
Received 25 February 2020
Received in revised form 24 June 2020
Accepted 23 July 2020
Available online 7 August 2020

Keywords:
Intensity-modulated proton therapy
Prostate cancer
Online-adaptive proton therapy
Online treatment planning
Robust treatment planning
Inter-fraction variation

ABSTRACT

Background/purpose: Intensity-modulated proton therapy (IMPT) is highly sensitive to anatomical variations which can cause inadequate target coverage during treatment. Available mitigation techniques include robust treatment planning and online-adaptive IMPT. This study compares a robust planning strategy to two online-adaptive IMPT strategies to determine the benefit of online adaptation.

Materials/methods: We derived the robustness settings and safety margins needed to yield adequate target coverage ($V_{95\%} \geq 98\%$) for >90% of 11 patients in a prostate cancer cohort (88 repeat CTs). For each patient, we also adapted a non-robust prior plan using a simple restoration and a full adaptation method. The restoration uses energy-adaptation followed by a fast spot-intensity re-optimization. The full adaptation uses energy-adaptation followed by the addition of new spots and a range-robust spot-intensity optimization.

Dose was prescribed as 55 Gy(RBE) to the low-dose target (lymph nodes and seminal vesicles) with a boost to 74 Gy(RBE) to the high-dose target (prostate). Daily patient set-up was simulated using implanted intra-prostatic markers.

Results: Margins of 4 and 8 mm around the high- and low-dose target regions, a 6 mm setup error and a 3% range error were found to obtain adequate target coverage for all repeat CTs of 10/11 patients (94.3% of all 88 repeat CTs).

Both online-adaptive strategies yielded $V_{95\%} \geq 98\%$ and better OAR sparing in 11/11 patients. Median OAR improvements up to 11%-point and 16%-point were observed when moving from robust planning to respectively restoration and full adaption.

Conclusion: Both full plan adaptation and simple dose restoration can increase OAR sparing besides better conforming to the target criteria compared to robust treatment planning.

Due to its characteristic Bragg Peak, intensity-modulated proton therapy (IMPT) can deliver dose locally, avoiding low dose baths and improving dose conformality. These Bragg Peaks however also make IMPT sensitive to anatomical variations such as changes in density, organ-shape and location [1–3]. Two mitigation strategies accounting for such uncertainties are robust treatment planning and online-adaptive IMPT. Robust treatment planning is a passive strategy which preemptively includes errors scenarios in the optimization possibly combined with safety margins to account for anatomical variations [4–6]. Conversely, online-adaptive IMPT is an active strategy taking the optimized plan and adapting it to better fit the daily anatomy and undo the effects of density variations prior to each fraction [7–13].

Making a treatment plan more robust inevitably results in increased doses to healthy tissues [14]. Conversely, online-adaptive planning aims at maintaining an adequate target volume coverage, while minimizing the dose to the organs at risk (OARs) for each fraction. In previous work, we developed online-adaptive treatment planning methods which are feasible for clinical implementation. Starting with the development of a dose restoration method [8], we could restore the initial dose distribution from a dose distribution distorted due to differences in density. Subsequently, we extended this into a full, but sufficiently fast, automated plan adaptation method to adapt the plan to the daily shape and position of the target volume and OARs [10,12]. We demonstrated that both methods can achieve acceptable target coverage for (most of) the fractions and simultaneously yield OAR doses close to what can be achieved with a fully optimized treatment plan generated without time constraints [8,10,12].

So far, however, the proposed adaptive treatments have not been compared to non-adaptive treatments for which robust treatment

* Corresponding author at: Erasmus MC Cancer Institute, Department of Radiation Oncology, Dr. Molewaterplein 40, 3015 GD Rotterdam, The Netherlands.
E-mail addresses: t.jagt@erasmusmc.nl (T.Z. Jagt), s.breedveld@erasmusmc.nl (S. Breedveld), r.vanhaveren@erasmusmc.nl (R. van Haveren), b.heijmen@erasmusmc.nl (B.J.M. Heijmen), m.hoogeman@erasmusmc.nl (M.S. Hoogeman).

https://doi.org/10.1016/j.radonc.2020.07.054
0167-8140/

planning is used to mitigate uncertainties in the daily patient anatomy. Such a comparison is complex, because although individual uncertainties such as intra-fraction motion and positioning variations have been described in literature, information on how to combine these in robustness settings and safety margins in robust optimization is still lacking. A comparison is nevertheless recommendable to establish the value of online-adaptive treatment approaches and to determine whether the benefits outweigh the costs.

In this work, we therefore evaluated the dosimetric benefit of the two developed methods for online-adaptive IMPT by comparing them to a robust treatment planning approach. To this end, we first derived the robustness settings and magnitude of the safety margins needed to yield adequate target volume coverage in a set of prostate cancer patients with repeat CT scans. Secondly, for each fraction we compared the online-adaptive approaches to the recomputed robust treatment plans in terms of target coverage and OAR dose.

Methods and materials

Patient data

This study included data of 11 prostate cancer patients, with 8–10 available repeat CT scans per patient selected from a phase II dose-escalation trial approved by the western Norway regional committee for medical and health research ethics (2006-15727). The original planning CT scans were excluded, as these were generated using contrast fluid, making dose calculation inaccurate. Taking instead the first repeat CT scan as planning CT scan (pCT), 88 repeat CT scans (rCTs) remained for evaluation. From here on, pCT refers to the first repeat CT scan being used as planning CT.

Treatment planning volumes and prescription

Dose was prescribed according to a simultaneously-integrated boost scheme comprising a high-dose region of 74 Gy(RBE) and a low-dose region of 55 Gy(RBE), to be delivered in 37 fractions, using an RBE of 1.1. An intermediate target dose-region, generated as the 15 mm transition between the high- and low-dose regions, was assigned a dose between 55 and 74 Gy(RBE) to steer dose fall-off. On each scan two clinical target volumes (CTVs) were delineated. For the high-dose region, a CTV_{High} was defined as the prostate, a CTV_{Low} was defined for the low-dose region as the lymph nodes and seminal vesicles. From here on we will denote the combination of the CTV_{High} and the CTV_{Low} as CTV. The rectum, bladder, small and large intestines, and the femoral heads were defined as OARs. Target delineations were available in all rCTs, OAR delineations in most. For scans missing the delineations of the intestines or femoral heads the pCT delineations were projected onto the rCT. Dose was to be delivered with two laterally opposed beams.

All rCTs were aligned to the corresponding pCT by a translation based on implanted intra-prostatic markers.

Both adaptation strategies require a prior treatment plan generated on the pCT to start the adaptation. These prior plans were generated using the PTV_{Prior} structures, which were generated by enlarging the CTV_{High} of the pCT by 7 mm, and the CTV_{Low} by 10 mm. Relatively large margins were selected to ensure sufficient spot coverage for most target deformations seen in the rCTs, as was done in previous work [10].

Mitigation strategies

Three mitigation strategies were compared in this study, all aiming for a clinically acceptable dose in all treatment fractions.

- *Strategy A – Robust treatment planning:* On each pCT a robust treatment plan was generated. To account for internal organ motion with respect to the daily alignment on the markers, targets were expanded by safety margins creating internal target volumes (ITVs). Subsequently, robust optimization was applied using the 'minimax' worst-case approach [4–6], including range robustness to account for uncertainties in the conversion from Hounsfield units to proton stopping power and including setup robustness to account for patient shifts relative to the daily alignment. Nine error scenarios were optimized simultaneously (nominal, ±setup, ±range). We derived the robustness settings and magnitude of the safety margins required for this dataset to ensure adequate coverage in all target regions of all rCTs for at least 90% of the patients. This was done by systematically increasing the margins (0–8 mm in steps of 2 mm) and the setup error (2–8 mm in steps of 2 mm), while evaluating the effect on the rCTs. The range error, related to uncertainties in the stopping power prediction, was fixed at 3%. For more details see the Supplementary Materials. CTV coverage of the rCTs was evaluated by a forward dose calculation of the robust treatment plan on each rCT.
- *Strategy B – Plan restoration:* For each rCT the dose distribution of the prior treatment plan, optimized on the pCT, was restored. This was done using the delineations of the pCT projected onto the rCT. The restoration method uses energy-adaptation followed by a fast spot-intensity re-optimization focusing on the targets. Details on this method can be found in [8]. Evaluation was done on the CTV structures of the rCTs.
- *Strategy C – Full plan adaptation:* For each rCT, the prior plan optimized on the pCT was used as a warm-start for adaptation. The method starts with an energy-adaptation, followed by adding 2500 new spots and a spot-intensity optimization using the Reference Point Method (RPM). To account for uncertainties in stopping power prediction the optimization is robust to a ± 3%-range. Adaptation is done based on the available contours in the rCTs. To account for inevitable segmentation errors as well as intra-fraction motion uncertainties, the CTV contours were expanded by small margins creating PTV_{OAPT} structures (Online-Adaptive Proton Therapy). As was done in previous work, a 2 mm margin was added around the CTV_{High} of the rCT and a 3.5 mm margin was added around the CTV_{Low} [10]. Parameter tuning for this strategy was done using three-fold cross validation, where one third of the patients (selected randomly) was used for tuning and the remaining two thirds for testing. Evaluation was done on all folds simultaneously, i.e. 176 plans (two per scan). A brief explanation of the RPM and the tuning is shown in the Supplementary Materials. Details on the full adaptation method can be found in [10,12]. Evaluation was done on the PTV_{OAPT} structures of the rCTs.

Note that evaluation of the three strategies is done on different target definitions, i.e. the daily CTVs for robust planning (A) and simple dose restoration (B) and the PTV_{OAPT} for full plan adaptation (C). This was done to include segmentation errors that are inevitable in an online-adaptive approach, thereby avoiding a too optimistic evaluation for strategy C.

The prior and robust treatment plans were generated using our in-house developed multi-criteria treatment planning system 'Erasmus-iCycle' combined with the 'Astroid' dose engine. All plans were optimized to obtain clinically acceptable target coverage defined as $V_{95\%} \geq 98\%$ while simultaneously aiming for $V_{107\%} \leq 2\%$ for their respective PTV and ITV. Here $V_{95\%}$ and $V_{107\%}$ are the percentages of the volumes receiving respectively 95% and 107% of the prescribed dose. Dose to the OARs was minimized according to the objectives shown in Table S1 (Supplementary Materials).

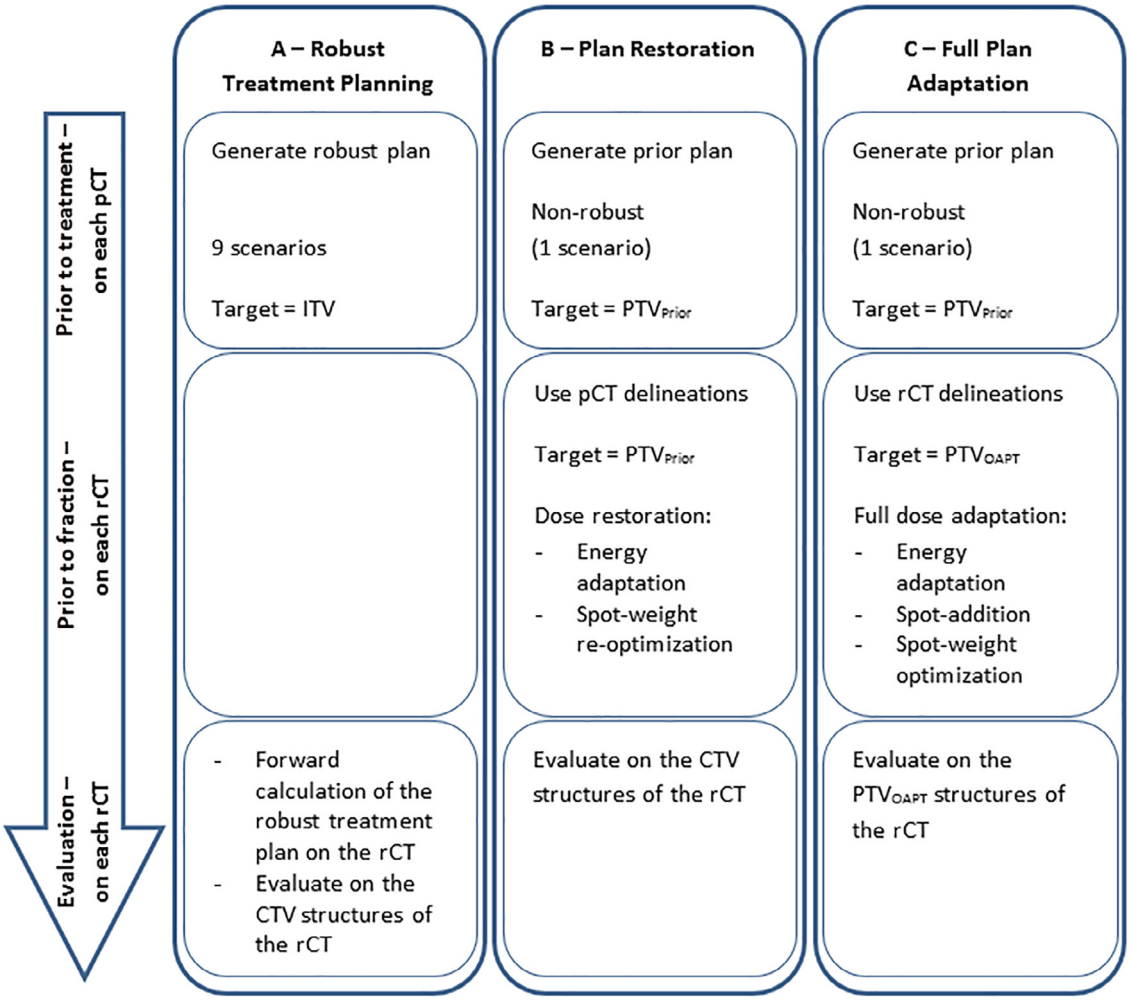

Fig. 1. Summary of the compared strategies.

More details can be found in [15–20]. Fig. 1 summarizes the compared methods.

Comparison and evaluation of the methods

For each rCT, the dose distributions obtained with the three strategies were checked visually and whether they fulfilled the targets planning criteria. We report the targets $V_{95\%}$, $V_{107\%}$ and $V_{110\%}$. In case of hotspots we also report the $D_{2\%}$ and D_{max}. For the rectum, we report the $V_{75Gy(RBE)}$, $V_{60Gy(RBE)}$, $V_{45Gy(RBE)}$, D_{mean} and $D_{2\%}$ and for the bladder the $V_{65Gy(RBE)}$, $V_{45Gy(RBE)}$, D_{mean} and $D_{2\%}$. For the whole body (patient) we report the$V_{10Gy(RBE)}$ and $D_{2\%}$. Here $V_{xGy(RBE)}$ is the percentage of the volume receiving x Gy(RBE), D_{mean} is the average dose and D_{max} is the maximum dose.

All calculations were performed on a dual Intel Xeon E5-2690 server.

Statistical analysis

Wilcoxon signed-rank tests were performed using MATLAB (Mathworks version 2017a) to evaluate the differences between the strategies. A p-value <0.05 was considered to be statistically significant.

Results

For robust treatment planning (A), expanding the CTV_{High} and CTV_{Low} with a 4 mm and 8 mm safety margin, respectively and applying a range error of 3% and a setup error of 6 mm to the targets during robust optimization yielded adequate target coverage ($V_{95\%} \geq 98\%$ for all target regions) for all rCTs in 10/11 patients. The other patient had $98\% > V_{95\%} \geq 95.5\%$ for the CTV_{Low} for 3/8 rCTs.

Applying the robust treatment plans on the rCTs resulted in a population-mean $V_{107\%}$ of the CTV_{Low} of 44.8% (19.5%–60.9%) and a population-mean $V_{110\%}$ of 19.9% (5.6%–37.6%). $D_{2\%}$ values up to 65.8 Gy(RBE) and D_{max} values up to 75.1 Gy(RBE) were obtained (respectively 119.6% and 136.5% of 55 Gy(RBE)). These high values are due to the proximity of the ITV_{High} and ITV_{Low}, as during robust optimization the dose in the ITV_{Low} is increased to achieve adequate ITV_{High} coverage in the error scenarios.

For the CTV_{High} all scans obtained $V_{107\%} \leq 2\%$ and $V_{110\%} = 0\%$. No combination of margins and robustness was found obtaining sufficient coverage for all target regions for all rCTs of all patients.

Applying plan restoration (B) yielded $V_{95\%} \geq 98\%$ for all scans. For the CTV_{High} all scans obtained $V_{107\%} \leq 2\%$, but for the CTV_{Low} 21/88 scans obtained $V_{107\%} > 2\%$, with values up to 3.7%. $D_{2\%}$

values up to 59.6 Gy(RBE) and D_{max} values up to 71.7 Gy(RBE) were obtained (respectively 108.4% and 130.4% of 55 Gy(RBE)). All 88 scans obtained $V_{110\%} = 0\%$ for the CTV_{High}, but $0\% < V_{110\%} < 1.6\%$ for the CTV_{Low}.

Applying the full plan adaptation method (C) yielded $V_{95\%} \geq 98\%$ for all plans for the PTV_{OAPT_High} and PTV_{OAPT_Low}. For the PTV_{OAPT_High} 54/176 plans obtained $V_{107\%} > 2\%$ (up to 37.3%) and 9/176 plans $V_{110\%} > 0\%$ (up to 15.2%). $D_{2\%}$ values up to 84.0 Gy(RBE) and D_{max} values up to 85.3 Gy(RBE) (respectively 113.5% and 115.3% of 74 Gy(RBE)) were obtained. For the PTV_{OAPT_Low} 20/176 plans obtained $V_{107\%} > 2\%$ (up to 13.7%), with $D_{2\%}$ and D_{max} values up to 59.9 Gy(RBE) (108.9% of 55 Gy(RBE)). All plans obtained $V_{110\%} = 0\%$.

In terms of OAR sparing the adaptive strategies (B and C) outperformed strategy A for all patients. Fig. 2 shows boxplots depicting the obtained OAR values for the three strategies. Largest differences between the strategies were observed for the $V_{45Gy(RBE)}$ of both rectum and bladder. For the rectum the median value improved with 11.1%-point when moving from robust treatment planning to plan restoration (A to B) and 16.3%-point when moving to full plan adaptation (A to C). For the bladder these improvements were respectively 6.9%-point and 9.9%-point. For the high dose criteria ($V_{75Gy(RBE)}$, $D_{2\%}$ and D_{max}) smaller differences between the strategies were observed. For all evaluation criteria of the OARs the differences between robust treatment planning (A) and plan restoration (B), as well as the differences between plan restoration (B) and full plan adaptation (C) were statistically significant.

Fig. 3 shows an example of a slice of the dose distributions obtained for one of the rCTs using the three different strategies. It can be seen that the high-dose region is largest for robust treatment planning (A) and smallest for plan adaptation (C).

Plan restoration (B) took on average 1.7 min (1.4–2.1) and full plan adaptation (C) took on average 6.6 min (5.0–9.8). These times include the adaptation steps and intermediate dose calculations, but exclude initialization and final dose calculation, thus reflecting the additional time required compared to recalculation of a static plan on the rCT (strategy A). For both methods, the initialization consumed on average ~1 min. The final dose calculation takes on average 3.9 min for plan restoration (2.1–5.5) and 7.0 min for full adaptation (3.1–11.3).

Discussion

In this study, robust treatment planning combined with safety margins (A) was compared to two adaptive strategies (B and C). Plan restoration and full plan adaptation both achieved $V_{95\%} \geq 98\%$ for all rCTs, while robust treatment planning did not meet this criteria for one patient. Applying adaptive treatment planning always resulted in lower OAR doses than robust treatment planning, with largest median improvements observed for the rectum (up to 16.3%-point). Several studies have shown OAR dose to be correlated to toxicity [21], so lowering these with online-adaptive IMPT can potentially reduce the expected toxicities compared to a strategy that fully relies on robust treatment planning.

For the robust treatment planning approach we derived required margins and robustness settings to achieve adequate target coverage for all rCTs in at least 90% of the patients. We obtained five combinations of margins and robustness settings all yielding adequate target coverage for all rCTs of 10/11 patients. For this study, we selected the combination with the smallest margins and robustness settings. It should be noted that these settings are specific to the investigated dataset and the number of robustness scenarios and have not been validated on other datasets. The observed benefit of adaptive planning likely depends on the dataset and robustness settings that are used.

In this study both targets were robustly optimized using the same values for setup and range robustness to stay close to clinical practice. More research is needed to determine whether OAR doses could be reduced by applying target-specific robustness settings. The effect of fractionation has not been considered in this study. Fractionation can potentially average out underdosage or overdosage in the target volume. Hence, the evaluation criteria applied in this study for the three strategies might be too conservative. However, while uncertainties in photon radiotherapy mostly result in dose deviations around the target-edges, IMPT can result in underdosage in the center of the target. Whether an underdosage in the center of the target volume can be effectively compensated by an overdosage in another fraction is unclear. Besides this, treatments are increasingly delivered in fewer fractions reducing the averaging effect [22].

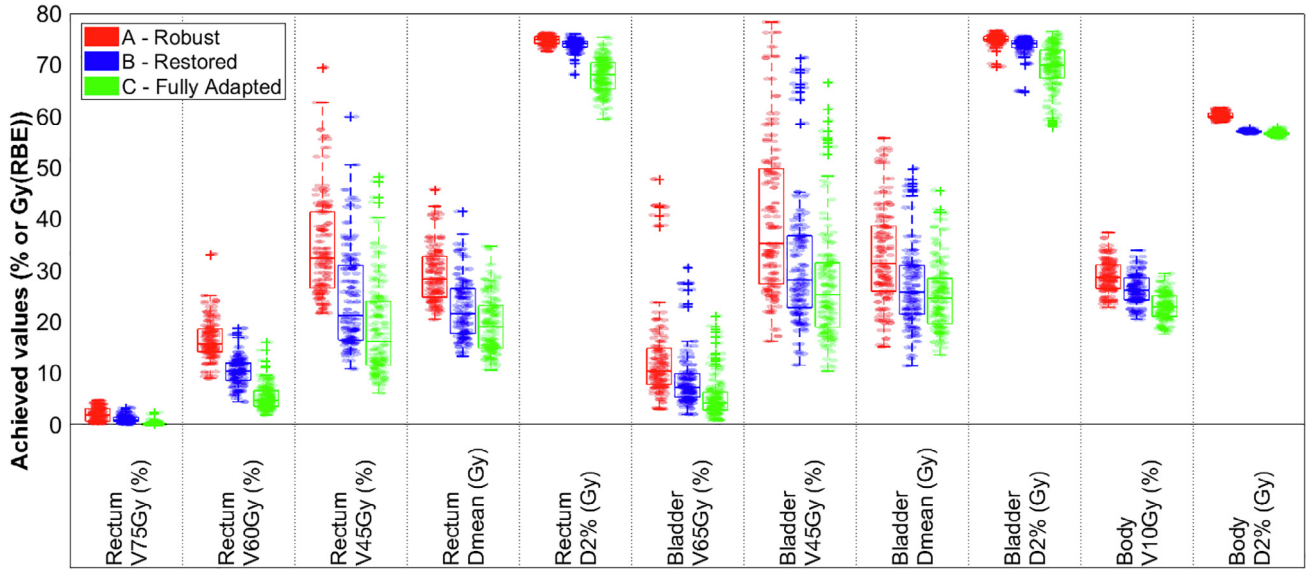

Fig. 2. Boxplots depicting the obtained dosimetric parameter values for the three strategies.

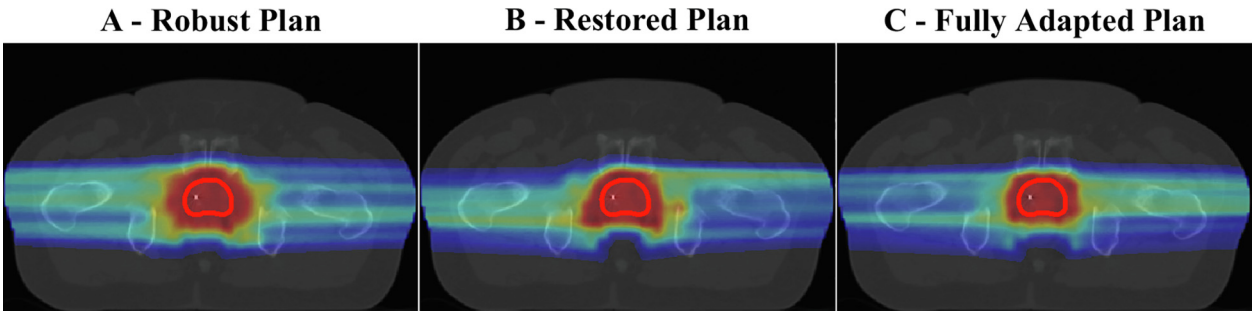

Fig. 3. An example of the dose distributions obtained using the different strategies for one repeat CT scan. The red contour indicates the daily CTV_{High}.

For the adaptation methods prior plans including large margins were used, as these have shown to be effective in previous work [10]. Changing these prior margins and changing the PTV_{OAPT} margins may influence the observed gain of adaptive planning. Furthermore, due to the used optimization method, the plans obtained through simple dose restoration are not explicitly made robust against range errors caused by uncertainties in stopping power prediction. While setup errors should be negligible in the daily adaptive workflow, range errors arising from Hounsfield Unit to proton stopping power conversion remain present. For full plan adaptation, we have therefore included range robustness in the spot-weight optimization. The tuning of the RPM-parameters however has been done without including range robustness. This could be an explanation for the elevated $V_{107\%}$ values obtained with full plan adaptation. Including range robustness in the tuning could possibly reduce these, although from a clinical perspective these values are acceptable.

In this study the three methods have been compared for a dataset of high-risk prostate cancer patients. This treatment group is interesting for online-adaptive planning due to the challenges which are related to the size of the target volume, its location in the pelvic region, and the differential motion between the low-dose and high-dose target volumes. Investigating the benefit of online-adaptive planning in other treatment sites such as head and neck cancer and locally advanced cervical cancer and lung cancer is part of ongoing and future research.

All treatment plans were made using two laterally opposed beams. While more complex beam geometries might improve all three methods, finding such a geometry requires further research. For all methods the CTs were aligned based on intra-prostatic markers. This approach may differ between centres. The accuracy of alignment might influence the required setup robustness and margins. However, as the alignment was the same for all methods, no effect on the comparison is expected.

Intra-fraction variations have not been addressed in this study. However, we included a small margin (2.0/3.5 mm) to account for the extra intra-fractional motion potentially occurring between the start of the full adaptation and beam delivery and to account for segmentation uncertainties. Intra-fraction motion during beam delivery was ignored for all three methods, but could easily be included by expanding the PTV or ITV or increasing robustness. Whether the included margins are sufficient or whether larger margins or more robustness is required was outside the scope of this study and should be investigated before clinical implementation.

General challenges of introducing online-adaptive IMPT into the clinic include adaptation time, user interaction time, the need for daily delineations and plan quality assurance (QA). Considering the adaptation time, the fully automated process now takes on average 2.9 min for dose restoration, and 7.5 min for full adaptation. As anatomical variations could occur during this time span, calculation times should be further reduced. The intermediate dose calculations are the most time consuming. Dose calculation time can be shortened considerably for example by parallelization and running the calculations on a GPU, as shown by Silva et al. [23,24] and Matter et al. [13]. This was however outside the scope of this study. Regarding the user interaction time, as both investigated adaptive strategies are fully automated, user interaction is only required once in advance to tune the parameters for an entire patient population, and once prior to each fraction to verify and approve the adaptation. The latter can be automated as well by automatically computing relevant dosimetric parameter values of the adapted plan and checking these against predefined limits. Prior to adaptation however the delineations of the rCT should be generated. When done manually, this step requires time-consuming user interaction. This can be largely avoided by (partly) generating the daily delineations automatically. For prostate cancer patients, an auto-propagation method combining deep-learning with deformable image registration has for example been developed with which already 80% of the automatically propagated pCT contours onto the rCT could be used without manual corrections [25]. Without deep-learning, contour propagation was used in for example the work on adaptive planning by Kurz et al. and Botas et al. [7,11]. Additional uncertainties in automatically generated contours can be accounted for by adding a margin to the targets as was done in the present study. It should be noted that daily delineations are only needed for full plan adaptation, as plan restoration uses the pCT contours. Another challenge lies in daily plan QA, for which little to no time is available in the daily adaptive workflow. This can be solved using alternatives such as a redundant dose calculation, online dose monitoring using prompt gamma emission profiles [26], and using machine log files [27,28] to verify the correct delivery of the treatment plan.

In conclusion, having demonstrated that plan adaptation in IMPT can reduce dose to OARs compared to robust treatment planning within a clinically acceptable time frame, we consider it auspicious to start exploring clinical implementation of online-adaptive strategies in IMPT.

Acknowledgements

The CT-data with contours were collected at Haukeland University Hospital, Bergen, Norway and were provided to us by responsible oncologist Svein Inge Helle and physicist Liv Bolstad Hysing. This study was financially supported by ZonMw, the Netherlands Organization for Health Research and Development, grant number 104003012 and by Varian Medical Systems.

Conflicts of interests

Varian Medical Systems has in part financed this research. Erasmus MC Cancer Institute also has research collaborations with Elekta AB, Stockholm, Sweden and Accuray Inc., Sunnyvale, USA.

Appendix A. Supplementary data

Supplementary data to this article can be found online at https://doi.org/10.1016/j.radonc.2020.07.054.

References

[1] Thörnqvist S, Muren LP, Bentzen L, Hysing LB, Høyer M, Grau C, et al. Degradation of target coverage due to inter-fraction motion during intensity-modulated proton therapy of prostate and elective targets. Acta Oncol 2013;52:521–7.

[2] Lomax AJ. Intensity modulated proton therapy and its sensitivity to treatment uncertainties 1: the potential effects of calculational uncertainties. Phys Med Biol 2008;53:1027–42. https://doi.org/10.1088/0031-9155/53/4/014.

[3] Lomax AJ. Intensity modulated proton therapy and its sensitivity to treatment uncertainties 2: the potential effects of inter-fraction and inter-field motions. Phys Med Biol 2008;53:1043–56. https://doi.org/10.1088/0031-9155/53/4/015.

[4] Fredriksson A, Forsgren A, Hårdemark B. Minimax optimization for handling range and setup uncertainties in proton therapy. Med Phys 2011;38:1672–84. https://doi.org/10.1118/1.3556559.

[5] Chen W, Unkelbach J, Trofimov A, Madden T, Kooy H, Bortfeld T, et al. Including robustness in multi-criteria optimization for intensity-modulated proton therapy. Phys Med Biol 2012;57:591–608. https://doi.org/10.1088/0031-9155/57/3/591.

[6] Fredriksson A, Bokrantz R. A critical evaluation of worst case optimization methods for robust intensity-modulated proton therapy planning. Med Phys 2014;41:081701. https://doi.org/10.1118/1.4883837.

[7] Kurz C, Nijhuis R, Reiner M, Ganswindt U, Thieke C, Belka C, et al. Feasibility of automated proton therapy plan adaptation for head and neck tumors using cone beam CT images. Radiat Oncol 2016;11. https://doi.org/10.1186/s13014-016-0641-7.

[8] Jagt TZ, Breedveld S, Van de Water S, Heijmen BJM, Hoogeman MS. Near real-time automated dose restoration in IMPT to compensate for daily density variations in prostate cancer. Phys Med Biol 2017;62:4254–72. https://doi.org/10.1088/1361-6560/aa5c12.

[9] Bernatowicz K, Geets X, Barragan A, Janssens G, Souris K, Sterpin E. Feasibility of online IMPT adaptation using fast, automatic and robust dose restoration. Phys Med Biol 2018;63:. https://doi.org/10.1088/1361-6560/aaba8c085018.

[10] Jagt TZ, Breedveld S, van Haveren R, Heijmen BJM, Hoogeman MS. An automated planning strategy for near real-time adaptive proton therapy in prostate cancer. Phys Med Biol 2018;63:135017. https://doi.org/10.1088/1361-6560/aacaa7.

[11] Botas P, Kim J, Winey B, Paganetti H. Online adaptation approaches for intensity modulated proton therapy for head and neck patients based on cone beam CTs and Monte Carlo simulations. Phys Med Biol 2019;64:. https://doi.org/10.1088/1361-6560/aaf30b015004.

[12] Jagt TZ, Breedveld S, van Haveren R, Nout RA, Astreinidou E, Heijmen BJM, et al. Plan-library supported automated replanning for online-adaptive intensity-modulated proton therapy for cervical cancer. Acta Oncol 2019. https://doi.org/10.1080/0284186X.2019.1627414.

[13] Matter M, Nenoff L, Meier G, Weber DC, Lomax AJ, Albertini F. Intensity modulated proton therapy plan generation in under ten seconds. Acta Oncol 2019;58:1435–9. https://doi.org/10.1080/0284186X.2019.1630753.

[14] van de Water S, van Dam I, Schaart DR, Al-Mamgani A, Heijmen BJM, Hoogeman MS. The price of robustness; impact of worst-case optimization on organ-at-risk dose and complication probability in intensity-modulated proton therapy for oropharyngeal cancer patients. Radiother Oncol 2016;120:56–62. https://doi.org/10.1016/j.radonc.2016.04.038.

[15] Breedveld S, Storchi PRM, Heijmen BJM. The equivalence of multi-criteria methods for radiotherapy plan optimization. Phys Med Biol 2009;54:7199–209. https://doi.org/10.1088/0031-9155/54/23/011.

[16] Breedveld S, Storchi PRM, Voet PWJ, Heijmen BJM. iCycle: Integrated, multicriterial beam angle, and profile optimization for generation of coplanar and noncoplanar IMRT plans. Med Phys 2012;39:951–63. https://doi.org/10.1118/1.3676689.

[17] Kooy HM, Clasie BM, Lu H-M, Madden TM, Bentefour H, Depauw N, et al. A case study in proton pencil-beam scanning delivery. Int J Radiat Oncol Biol Phys 2010;76:624–30. https://doi.org/10.1016/j.ijrobp.2009.06.065.

[18] Voet PWJ, Dirkx MLP, Breedveld S, Fransen D, Levendag PC, Heijmen BJM. Toward fully automated multicriterial plan generation: a prospective clinical study. Int J Radiat Oncol Biol Phys 2013;85:866–72. https://doi.org/10.1016/j.ijrobp.2012.04.015.

[19] van de Water S, Kraan AC, Breedveld S, Schillemans W, Teguh DN, Kooy HM, et al. Improved efficiency of multi-criteria IMPT treatment planning using iterative resampling of randomly placed pencil beams. Phys Med Biol 2013;58:6969–83. https://doi.org/10.1088/0031-9155/58/19/6969.

[20] van de Water S, Kooy HM, Heijmen BJM, Hoogeman MS. Shortening delivery times of intensity modulated proton therapy by reducing proton energy layers during treatment plan optimization. Int J Radiat Oncol Biol Phys 2015;92:460–8. https://doi.org/10.1016/j.ijrobp.2015.01.031.

[21] Landoni V, Fiorino C, Cozzarini C, Sanguineti G, Valdagni R, Rancati T. Predicting toxicity in radiotherapy for prostate cancer. Physica Med 2016;32:521–32. https://doi.org/10.1016/j.ejmp.2016.03.003.

[22] Widmark A, Gunnlaugsson A, Beckman L, Thellenberg-Karlsson C, Hoyer M, Lagerlund M, et al. Ultra-hypofractionated versus conventionally fractionated radiotherapy for prostate cancer: 5-year outcomes of the HYPO-RT-PC randomised, non-inferiority, phase 3 trial. Lancet 2019;394:385–95. https://doi.org/10.1016/S0140-6736(19)31131-6.

[23] da Silva J, Ansorge R, Jena R. Sub-second pencil beam dose calculation on GPU for adaptive proton therapy. Phys Med Biol 2015;60:4777–95. https://doi.org/10.1088/0031-9155/60/12/4777.

[24] Da Silva J, Ansorge R, Jena R. Fast pencil-beam dose calculation for proton therapy using a double-gaussian beam model. Front Oncol 2015;5:281. https://doi.org/10.3389/fonc.2015.00281.

[25] Elmahdy MS, Jagt T, Zinkstok RT, Qiao Y, Shahzad R, Sokooti H, et al. Robust contour propagation using deep learning and image registration for online adaptive proton therapy of prostate cancer. Med Phys 2019;46:3329–43. https://doi.org/10.1002/mp.13620.

[26] Lens E, Jagt TZ, Hoogeman MS, Schaart DR. Correlations between the shifts in prompt gamma emission profiles and the changes in daily target coverage during simulated pencil beam scanning proton therapy. Phys Med Biol 2019;64:. https://doi.org/10.1088/1361-6560/ab145e085009.

[27] Winterhalter C, Meier G, Oxley D, Weber DC, Lomax AJ, Safai S. Log file based Monte Carlo calculations for proton pencil beam scanning therapy. Phys Med Biol 2019;64:. https://doi.org/10.1088/1361-6560/aaf82d035014.

[28] Johnson JE, Beltran C, Wan Chan Tseung H, Mundy DW, Kruse JJ, Whitaker TJ, et al. Highly efficient and sensitive patient-specific quality assurance for spot-scanned proton therapy. PloS ONE 2019;2:. https://doi.org/10.1371/journal.pone.0212412e0212412.